

We are IntechOpen, the world's leading publisher of Open Access books Built by scientists, for scientists

6,200

Open access books available

168,000

International authors and editors

185M

Downloads

Our authors are among the

154

Countries delivered to

TOP 1%

most cited scientists

12.2%

Contributors from top 500 universities



WEB OF SCIENCE™

Selection of our books indexed in the Book Citation Index
in Web of Science™ Core Collection (BKCI)

Interested in publishing with us?
Contact book.department@intechopen.com

Numbers displayed above are based on latest data collected.
For more information visit www.intechopen.com



Chapter

Metamaterial Applications in Modern Antennas

*Mohamed Lashab, Mounir Belattar, Sekkache Hocine
and Halfaya Ahmed*

Abstract

The chapter presents different types of metamaterials, their historical evolution, physical properties, and applications in antennas design. Metamaterials are artificial structures that offer electric and magnetic properties that are not found in nature, such as negative permittivity and negative permeability. These properties are used in antennas design in order to obtain ultrawide bandwidth, high gain, and electrically small structures. Modern wireless mobile communication uses 5G technology and multi-input multi-output (MIMO) antennas, which are based on high-frequency transmission and ultrawide band. Metamaterials are very good candidate for this technology, where miniaturized antennas loaded with metamaterials structures are used. Recently, electromagnetic sensors were used for liquid identification in biological and medical substances based on metamaterials for the sake of high sensitivity and better classification. Different metamaterial types are used in these sensors, depending on the nature of liquid and the associated application.

Keywords: antennas, metamaterials, wideband, mobile

1. Introduction

Modern antenna design and fabrication are based on the suitable choice of the substrate material, technology of fabrication, and domain or type of application [1]. Generally, the choice of substrate material has an effect on the frequency range, losses reduction, and polarization mode or harmonics generation [2]. This chapter is concerned with the second and third point of antenna design, technology of fabrication, and the type or domain of application.

There are various techniques or technologies of fabrication of electromagnetic structure in general, and each one of them has specific interest and can be used for given application [3]. For instance, dielectric antennas resonators, known as DRA, are generally used to generate specific harmonics and propagation mode, on the top surface of the antenna, where various types of dielectrics are used [4]. The substrate-integrated waveguide (SIW) is a type of antenna where a waveguide is built on the top of the substrate, and the main advantages of these antenna are lower losses and better power handling [4, 5]. The metamaterial antennas (MTMs) are based on artificial materials that have uncommon physical properties, such as negative permittivity or

negative permeability; these types of antennas have many advantages, such as higher gain, wideband of frequency, and miniaturization effect [6].

Antenna design depends also on the domain of application, in this chapter electromagnetic sensors loaded with metamaterial are treated, and the higher sensitivity is obtained for dielectric identification of the ethanol liquid [7]. Compensated right-left hand (CRLH) structure is a special type of MTM, which is used to improve the sensitivity, and other structures of metamaterial are also used [8].

Metamaterials are artificial materials that are not found in nature, they are fabricated by special design of copper on any dielectric substrate [4]. Based on the principle of transmission lines (TLs), the early researchers have worked hard to find the first type of MTM known as split ring resonator (SRR), CSRR as complementary split ring resonator, and CLL as capacitive-loaded loop [9].

2. Historical development of metamaterials

The history of metamaterials started from artificial dielectric fabrication as microwave structures, and they were manufactured just after the Second World War [10], although the exploration of the artificial materials has started by the end of the nineteenth century. The first studies on metamaterials started in 1904, and these studies were carried out until the twentieth mid-century; all the research work done on this period was dealing with the phase velocity, group velocity, the pointing vector, and the wave vector [11]. In 1952, Kock, Rotman, and Schelkunoff started working on artificial dielectric [12], and they suggested magnetic particles made by capacitive-charged loops, the research aimed to obtain very high permeability. Further research work led to obtain completely modified dielectric, with desired permittivity and desired permeability; hence, the medium is considered as metamaterial [13].

Horace Lamb and Arthur Schuster [14] in their theoretical study approved the possibility of negative phase velocity accompanied with anti-parallel group velocity, and unfortunately, the experimental work was not done. In 1945, Leonid Mandelstam studied in detail the anti-parallel phase and the velocity group and proved possibility of negative velocity group in crystalline medium.

The first theoretical model of so-called metamaterial medium was examined by Veselago in 1967; due to lack of suitable materials and technical problems, the experimental work was delayed till the end of 1990. Veselago was the first to predict the reversed electromagnetic phenomena including the index of refraction; he invented the term “left-hand material” and studied the material with double-negative dielectric parameters, permeability, and permittivity; he published his famous paper in 1968 and gained the Nobel Prize [15].

John Pendry in 2000 presented the first practical research work based on metallic periodic structures as concentric shapes, called split ring resonator (SRR); his experimental results confirmed the theory proposed by Veselago. Indeed, he obtained negative permeability and negative permittivity around the resonant frequency of the SRR, and the negative index of refraction was also obtained by making specific combination of copper wires and cells [16]. He succeeded in modifying the magnetic structure of any material, only by providing SRR structures on the top of the material.

In 2003, Caloz and Itoh presented their first work on metamaterials based on transmission lines (TLs) [17–19], and they introduced a new microwave technology, namely the zero-order resonators (ZORs), based on composite right-left hand (CRLH) structures, considered as metamaterials. The CRLH technology is based on a

combination of right-hand (RH) and left-hand (LH) electric equivalent circuits, leading to a resonant frequency of the microwave structure independently of its dimension [19]. In 2006, Nader Engheta and Richard W. Ziolkowski [20] published their first investigation on physical aspect of metamaterials, and they presented theoretical development on different types of metamaterials, single-negative (SGN) and double-negative (DNG) medium, plus some applications on antennas.

3. Physical properties of metamaterials

3.1 Metamaterial definition

Metamaterials ("MTMs") are generally defined as homogeneous electromagnetic structures with unusual properties that are not available in nature [21]; homogeneous structure is also defined as structure with average size of the unit cell much smaller than the wavelength applied on this unit cell [22]. By taking into account this condition, the relationship that relates the effective parameters, known as the effective electric permittivity ϵ_{eff} and the effective magnetic permeability μ_{eff} and the index of refraction n , is given by the following equation.

$$n = \sqrt{\pm \epsilon_{\text{eff}} \mu_{\text{eff}}} \quad (1)$$

In all types of metamaterials, the value of the constitutive parameters permittivity and permeability depend on the mutual space between cells, also on the geometrical shape of the unit cell. The desired constitutive parameters are obtained once the cell shape and the spacing are predefined; generally, the cells are implemented on planar substrate, and the dielectric of the substrate can affect greatly the constitutive parameters [23].

Materials are generally classified into four categories as shown in **Figure 1**: the first region is for double-positive (DPS), where the permeability and the permittivity are

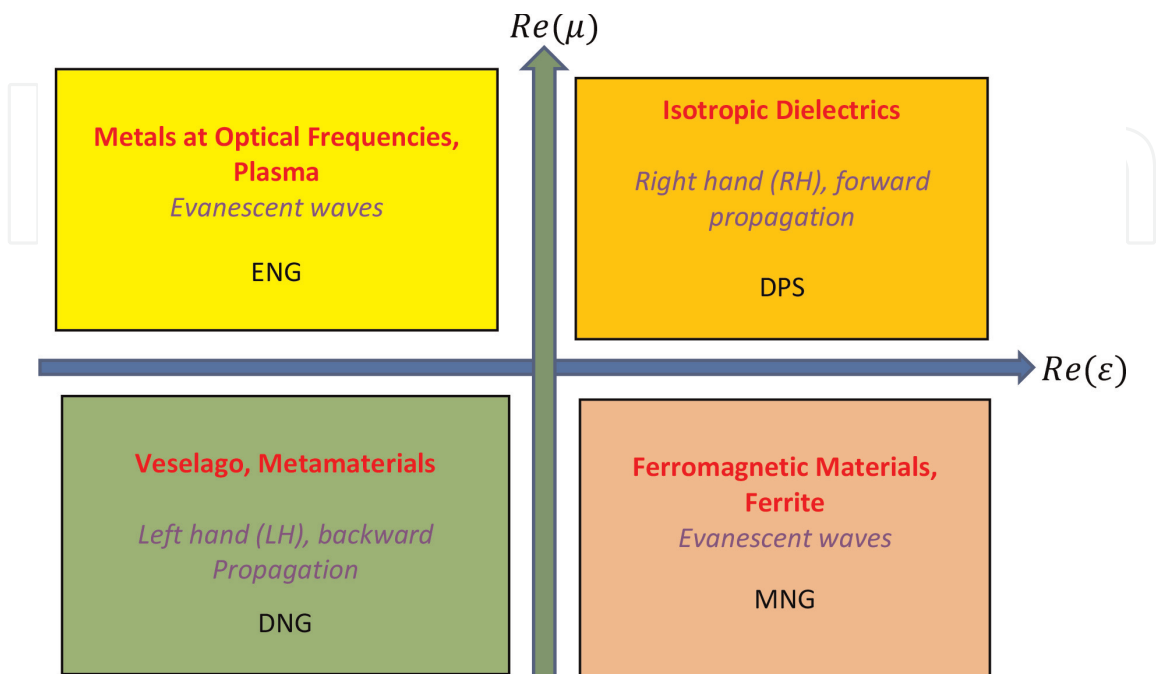


Figure 1.
 Material classification.

both positive; this region is known for isotropic dielectrics, right-hand (RH) materials; the second region is for permittivity negative, ENG region, considered as metamaterial region, realized with parallel plates or wires; the third region is for double-negative parameters (DNG); both the permittivity and permeability values are negatives; this region is for materials known as left-hand (LH) materials.

The last region is for permeability negative (MNG), and this region is for ferromagnetic and ferrite materials, generally fabricated from SRRs. In all regions near the zero axes, ENZ (ϵ near zero) and MNZ (μ near zero), both cases lead to ZIM (zero index metamaterial) [24].

3.2 Theoretical aspect of the SRR

Split ring resonators (SRRs) are artificial materials, and their permittivity and the permeability are not known; they vary with respect to the operating frequency, and the constitutive parameters are extracted either by experimental tests or by analytical models [25]. One of the well-known analytical methods is Drude-Lorentz model [26–28], known as the dispersion model, and this is a very accurate analytical method used to extract the constitutive parameters for unknown structures. For the split ring resonator or complementary SRR, **Figure 2**, using Drude-Lorentz model, the magnetic permeability and electric permittivity are described as follows:

$$\mu_r = \mu_0 \left(1 + \frac{F_u f^2}{f^2 - f_{ou}^2 + j\gamma f} \right) \quad (2)$$

And,

$$\epsilon_r = \epsilon_0 \left(1 + \frac{F_e f^2}{f^2 - f_{oe}^2 + j\gamma f} \right) \quad (3)$$

where ϵ_0 and μ_0 are respectively the background permittivity and the background permeability, whereas F_e and F_u are respectively the electric resonant intensity and the magnetic resonant intensity.

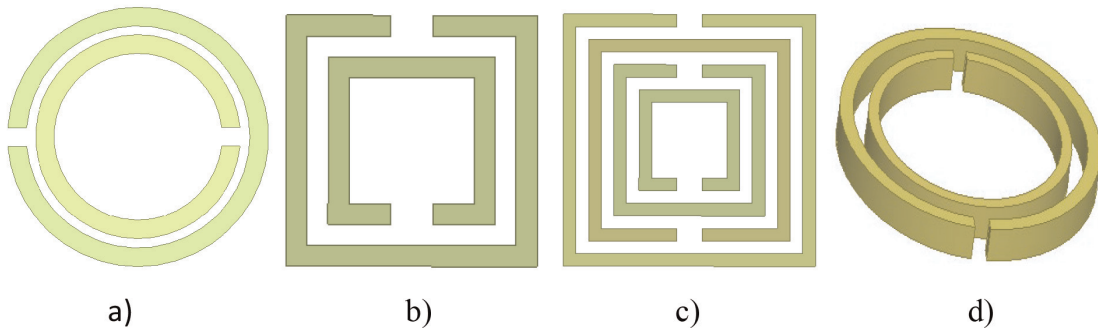


Figure 2. Schematic representation of different types of elementary unit cell structures of SRRs: (a) double-circular SRR, (b) double-square SRR, (c) multi-square SRR, (d) double-cylindrical SRR.

We define also f_{oe} as the electric resonant frequency and f_{ou} the magnetic resonant frequency, the parameter γ is the damping factor of the resonance; several technics or algorithms are used to calculate all these parameters, for given frequencies [29].

3.3 CRLH resonator

The CRLH resonator is based on transmission line (TL) structures, which is essential to realize any resonant planar antenna with no dependence on its physical dimension, and this structure supports an infinite wavelength at its fundamental mode, which is required to realize ZOR resonators [30]. A practical realization of a left-hand (LH) material includes unavoidable right-hand (RH) effects, and the CRLH resonator is able to support an infinite wavelength ($\beta = 0$, with $\omega \neq 0$) and therefore, can be used to realize any planar microwave structures [31].

The equivalent circuit model of the CRLH unit cell is shown in **Figure 3**, as “T” shape. The resonance condition of such open-ended resonator is given by the dispersion relation given below [32].

$$\beta = \frac{n\pi}{l}(0, \pm 1, \dots, \pm(N - 1)) \quad (4)$$

where “ l ” is the physical length of the resonator, n is the mode number, and N is the number of unit cells used to realize the CRLH, the equivalent electric circuit of a single unit cell is given by **Figure 3**, the electrical circuit contains an impedance Z and an admittance Y .

When the unit cell of zero-order resonator is inserted into the microwave structure, the size of this latter can be reduced since the resonant frequency does not depend on the physical dimension. In the case of open boundary conditions, the infinite wavelength resonance depends on the shunt parameters of the unit cell, the resonant frequencies are given by:

$$\omega_{sh} = \frac{1}{\sqrt{L_L C_R}} \text{ and } \omega_{ch} = \frac{1}{\sqrt{L_R C_L}} \quad (5)$$

where ω_{sh} is the shunt resonant frequency and ω_{ch} the serial resonant frequency [32]. More complicated zero-order structures than those given in **Figure 3** can be used, such as “Pi” shape or “T” shape, where the input and output have symmetrically the same components as in [33]; combination of the two types of shapes “T” and “Pi” can be employed to obtain more than two resonant frequencies [34].

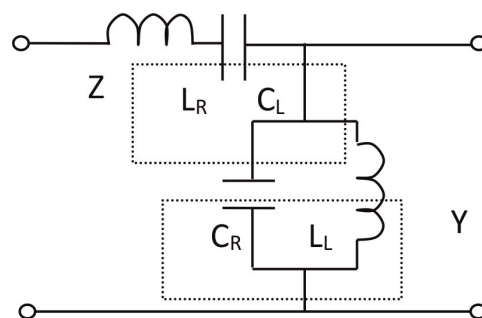


Figure 3.
 Equivalent electric circuit of the proposed CRLH.

4. Antennas based on metamaterials

4.1 Antenna description

A monopole antenna loaded with CRLH resonator used for LTE and WiMax application is presented in this section, and the CRLH unit cell is designed by a zigzag resonator that is inserted between two symmetrical parts, with bow-tie shapes of the monopole antenna [33]. An inter-digital capacitor in terms of zigzag slot is also incorporated inside the lower part of the monopole antenna to support the miniaturization process, **Figure 4**. The proposed antenna exhibits the UWB and the miniaturization effect along with an improvement of the gain and the bandwidth subject to optimize the process of CRLH structure. The achieved results of the loaded monopole with CRLH show that the antenna is covering an operational bandwidth of 1.8–2.15 GHz as LTE band, 4.0–6.5 GHz as WiMax band, and 6.8–12.15 GHz as X band.

For more than 20 years ago, published research work on monopole antennas was mainly dealing with applications related to microwave devices, and this is mostly due to the low cost of fabrication of these types of antennas, and in addition, they were very basic. However, the early research studies on these antennas were not subject to improvement regarding their performances such as the high gain and large bandwidth [33]. More interesting research works published recently on monopole antennas loaded with artificial materials or dielectrics have shown that these antennas brought great improvement on the gain and bandwidth, which make them good candidates for modern communication devices [34]. Generally, antennas loaded with metamaterials have very important performances, but in the literature, it has been shown that antennas loaded with resonant structures such as the SRRs are lossy with narrow bandwidth and not suitable for microwave applications. For instance, LHM structures (left-hand metamaterials) based on TL (transmission line) have wider bandwidth and lower losses [18].

Microwave structures loaded with CRLH are generally based on the insertion of inter-digital capacitors and shorted stub inductors inside the antenna or the sensor, by suitable choice of the components dimensions, and one can have desired resonant frequency [30]. It has been shown that by increasing the shunt and inductors, the

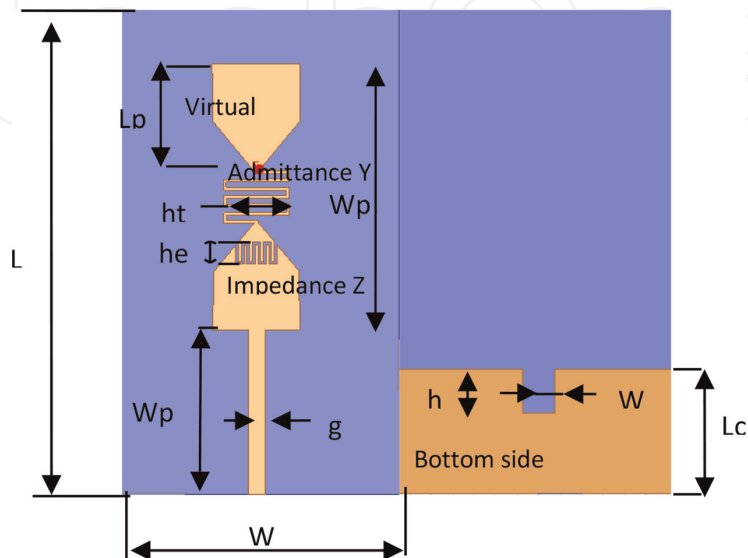


Figure 4. Geometrical dimension of the proposed antenna, front and bottom.

antenna size can be made much smaller. In this proposed structure, the shunt inductance is accomplished by embedding a chip inductor on one of the strips of the monopole antenna, and thus, it omits the need for vias to the ground. Inter-digital capacitor and virtual ground have been widely used in radio frequency application; for instance, small resonators are one of these applications [31].

In the literature, most of the research works have shown that structures loaded with ZOR-TL are used to make any antennas or microwave sensors as electrically small, they will appear electrically large. ZOR-TL technique is used to improve the antennas matching and achieve good radiation properties or better microwave structures. This technique could be implemented on any antennas by producing a zero-phase constant for a nonzero frequency, which means the wavelength of the traveling wave becomes infinite on the ZOR-TL. This is the most important technique, which makes the resonance condition completely independent from the physical dimensions of the microwave structure [30, 32]. This technique can be used to design miniaturized antennas for any microwave structure, and the resonance of such microwave devices for any operating frequency depends only on the CRLH characteristics to acquire ZOR at that frequency and nothing to do with the physical dimensions of the antenna.

4.2 Results and discussion

The proposed antenna is presented in **Figure 4**, the substrate is an FR4 with relative permittivity 4.4 and dielectric loss tangent 0.02, the thickness of the substrate is 1.6 mm, and geometrical dimensions are given in **Table 1**. The proposed antenna is constituted by top metallic patches as the radiating parts plus a defected ground on the bottom side of the antenna, to achieve a good impedance matching to 50 Ω , and the proximity coupling is used as the feed network. Two parts are added as CRLH components: first, the zigzag strip considered as admittance Y, and an inter-digital capacitor considered as the Z impedance. The upper part of the antenna contains a virtual ground, whereas the down part contains a defected ground; by this description, the equivalent electric circuit of the monopole antenna is exactly the electric circuit given in **Figure 3**.

Several types of antenna structures were investigated as shown in **Figure 5**, and the figure shows three types of antennas: the original antenna, antenna 2, and antenna 3. The reflection coefficients of the proposed antenna including the three prototype antennas given in **Figure 5** are presented in **Figure 6**. The figure presents two resonant frequencies corresponding exactly to ω_{sh} and ω_{ch} in which these frequencies are independent from the antenna size. For all the prototype antennas, the first resonant frequency is around 5.5 GHz, and the second one is around 11.12 GHz; it is remarkable that these frequencies can be shifted just by changing the ZOR shape.

L	W	Lp	Wp	ht
40	26	9.5	15	6
Lc	he	Wt	h	g
11.55	2	3	4	1.5

Table 1.
 Parameters of the proposed antenna in mm.

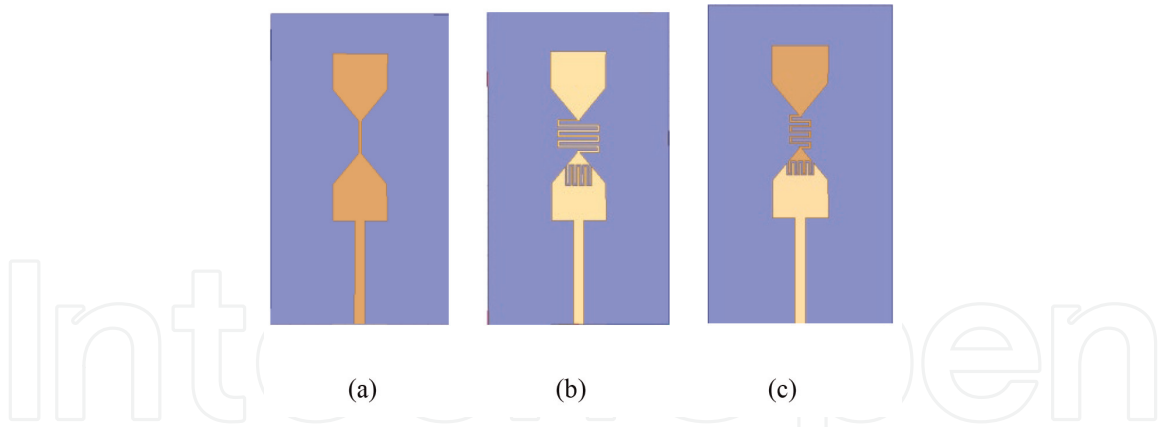


Figure 5. Three types of antennas: (a) original antenna , (b) antenna 2, $h_e = 3 \text{ mm}$, (c) Antenna 3, $h_t = 3 \text{ mm}$.

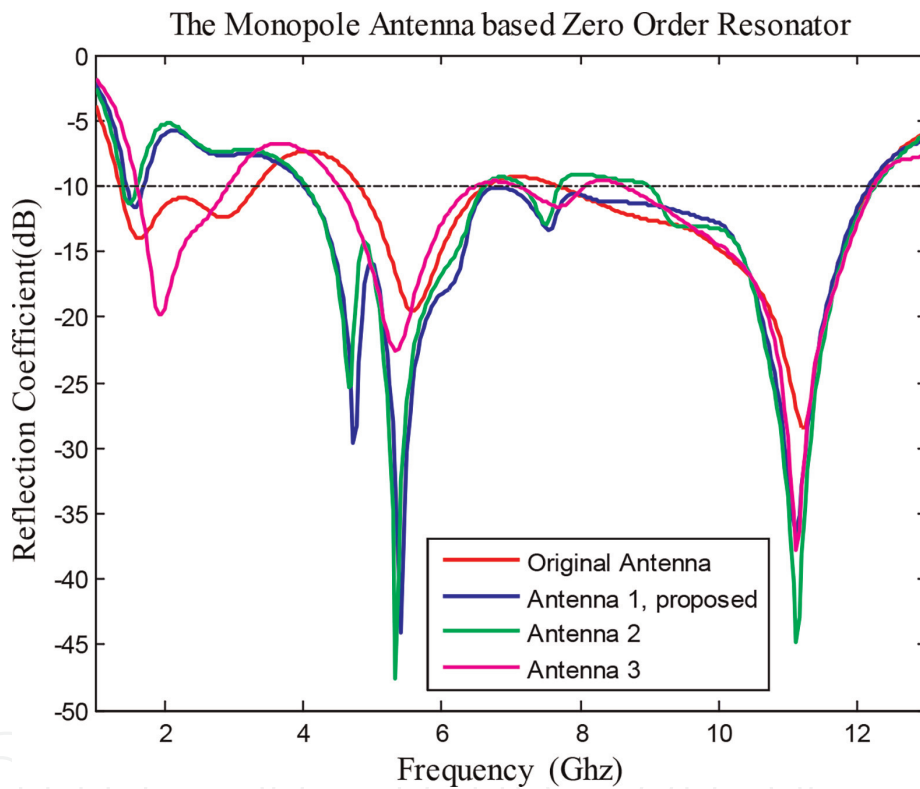


Figure 6. Reflection coefficients for different types of antennas.

The bandwidth of the proposed antenna is $12.15\text{GHz} - 4\text{GHz} = 8.15 \text{ GHz}$, which is nearly 148% impedance bandwidth. Since the gain and radiation pattern of antenna 1 and antenna 2 are similar, we confirm that the variation of the capacitance value in antenna 2 is more significant than the variation of inductor length in antenna 3. The radiation pattern in the xz -plane given in **Figure 7** shows that there is an improvement for the case of antenna1 and antenna 2, which is from -3 dBi to 1.4 dBi at frequency 5.5 GHz compared with the original antenna. It was also noticed that there is a slight increase of gain values concerning antenna 3 from -3 dBi to -2.5 dBi .

The radiation pattern in the yz -plane given in **Figure 8** presents a very remarkable improvement of the gain values of antenna 1 and antenna 2 at 5.5 GHz , which is 1.8 dBi compared with the original antenna, that is, -3 dBi . Antenna 2 and antenna 1 have almost the same improvement in the gain, but antenna 1 has a larger bandwidth.

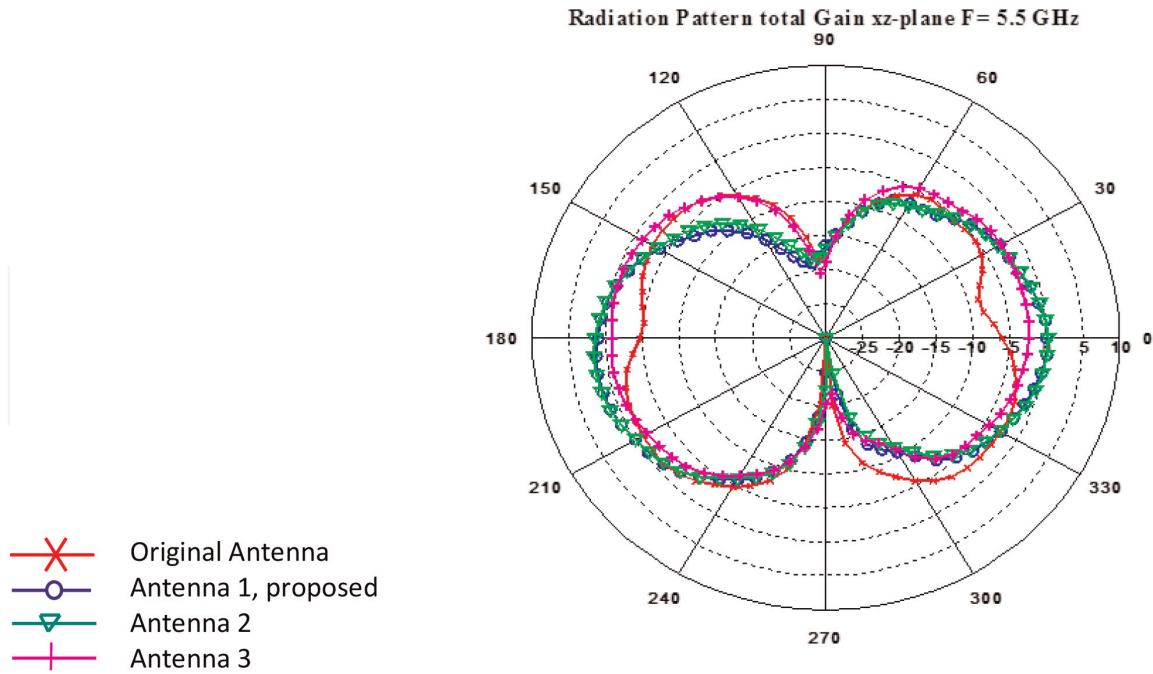


Figure 7.
Total gain radiation pattern in the xz-plane, $F = 5.5$ GHz.

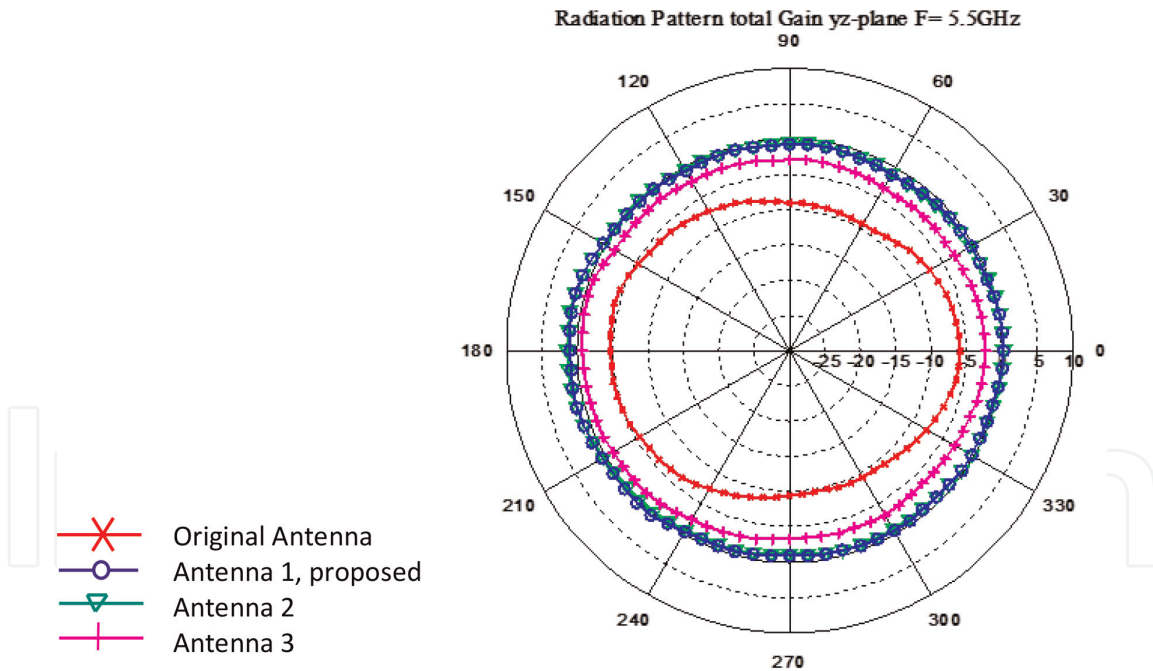


Figure 8.
Total gain radiation pattern in the yz-plane, $F = 5.5$ GHz.

5. Electromagnetic sensors based on metamaterial

5.1 Theoretical aspect

The main parts of the proposed sensor are the CRLH unit cell on the front side and the CSRR on the ground plane side, **Figure 9**. The sensor can be simulated and then optimized using the full-wave simulator Ansys HFSS.

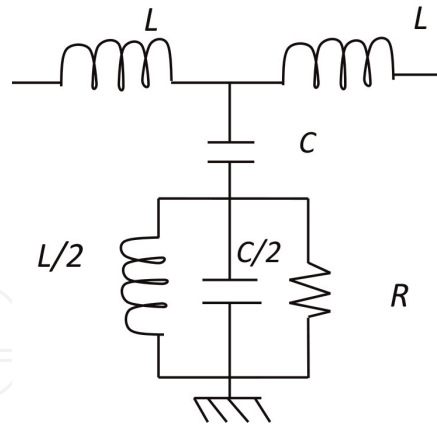


Figure 9.
Equivalent circuit of the proposed sensor, bottom view.

The equivalent electric circuit of the proposed sensor is the top side in **Figure 3**, whereas the equivalent electric circuit of the bottom side is given in **Figure 9**. In the CRLH unit cell, the impedance Z provides a series resonator based on (L_R, C_L) , whereas Y admittance provides a parallel resonator based on (L_L, C_R) [30–38].

5.2 Geometrical dimensions of the sensor

The proposed sensor is presented in **Figure 10a**, the substrate is an FR4 with relative permittivity 4.4 and dielectric loss tangent 0.02, the thickness of the substrate is 1.6 mm.

The sensor is composed of CRLH and CSRR circuits with two ports, the sensor presents a coplanar structure, grounded at the bottom side, the bottom ground is first filled with PEC ground and then with CSRR, and this is given in **Figure 10b**.

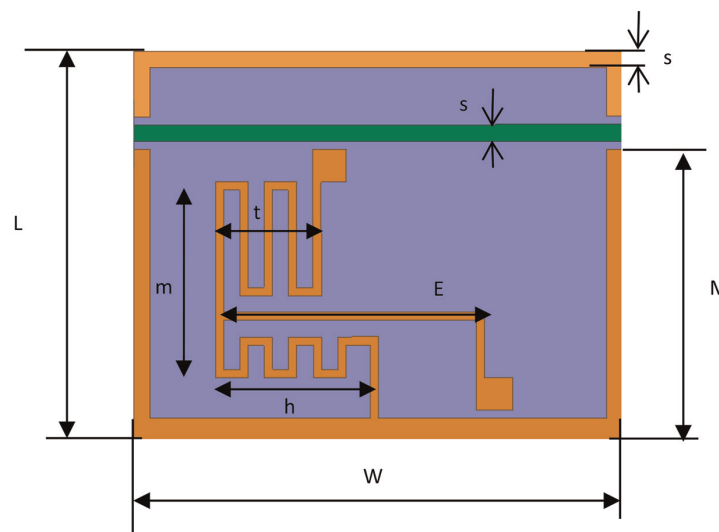
The proximity coupling is used as the feed network to achieve a good impedance matching to 50 Ω , the geometrical dimensions are given in **Table 2**.

5.3 Results and discussion

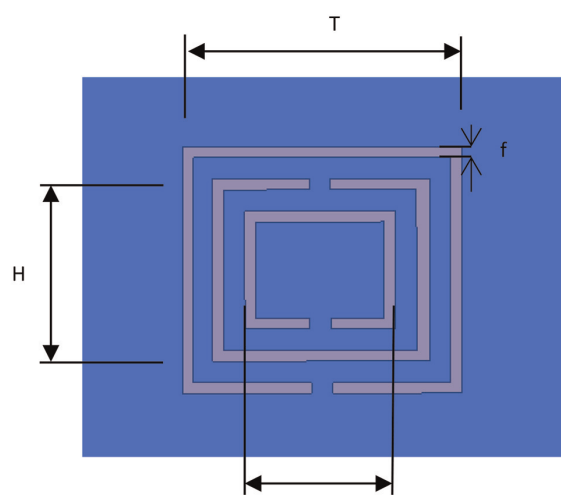
The transmission coefficient of the sensor without liquid mixture (air) is presented in **Figure 11**, and the figure shows three types of liquid plus the air (without liquid).

The substances are ethanol, methanol, distilled water, and air, and their resonant frequencies are, respectively, 1.06 GHz, 1.01 GHz, 0.92 GHz, and 1.22 GHz. The aim of this work is to load the sensor with different volume fraction of ethanol, the measured resonant frequencies enable the calculation of the sensor sensitivity, and the transmission coefficient of different volume fraction is presented in **Figure 12**; in this figure the response of air is missing.

The frequency range of the sensor is from 1.065 GHz to 1.195 GHz, a difference is of 0.13 GHz. The transmission coefficient of the sensor loaded with CSRR is given in



(a)



(b)

Figure 10.
 (a) Top view, (b) bottom view of the electromagnetic sensor, CSSR.

L	W	H	E	M	T
15	15	6	8	8.25	7.5
h	s	t	m	f	g
6.75	0.5	4.5	7	0.25	4.5

Table 2.
 Parameters of the proposed sensor in (mm).

Figure 12, there is a remarkable difference in higher volume fraction and almost none in the lower volume fraction. The liquid under test is presented in **Figure 13**, the liquid is supposed to be placed on the top of sensor in circular shape, and the input port and the output port are on the same side as shown in the figure.

Liquid identification of Ethanol, Methanol, Distilled water and Air, Sensor 1

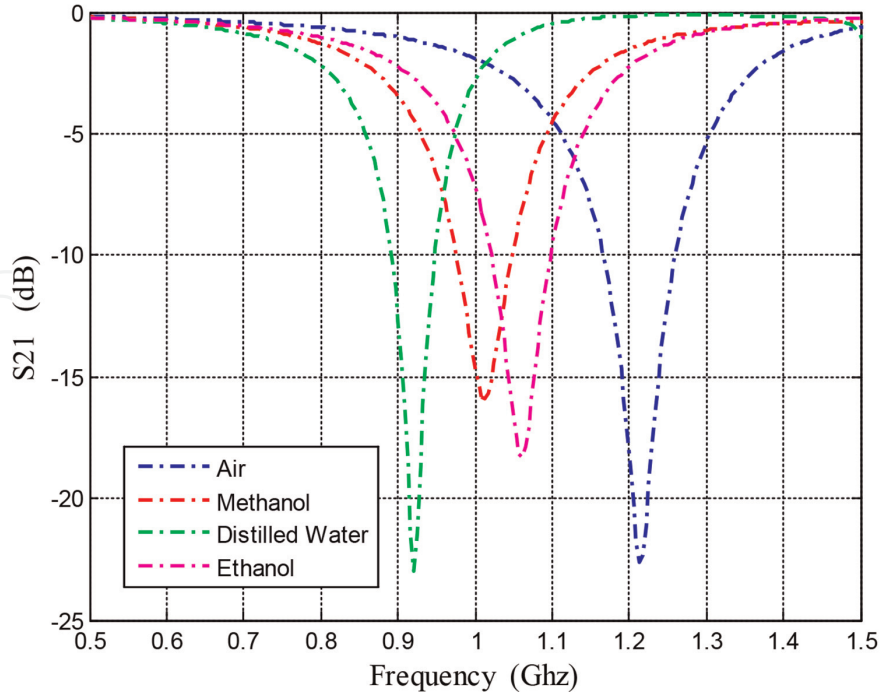


Figure 11.
Transmission coefficient with and without CSRR.

Sensor Liquid identification of Ethanol Based CRLH, Sensor 1

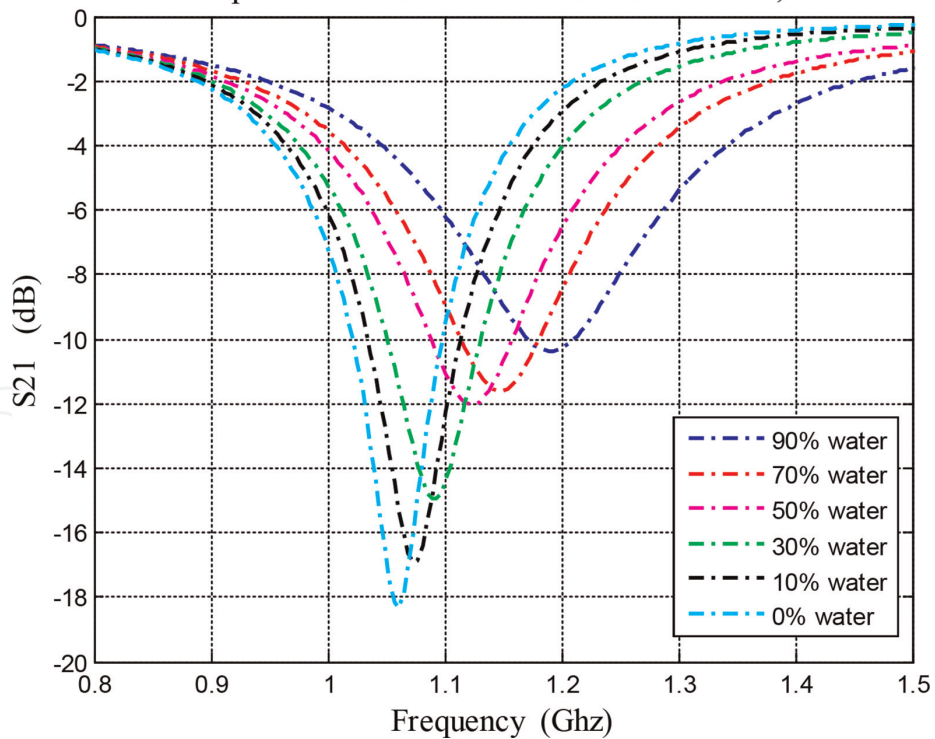


Figure 12.
Transmission coefficient of the volume fraction of ethanol.

According to the Debye relaxation model, the real part of the mixture permittivity can be expressed as follows [37–41]. Where ϵ_s is the low-frequency permittivity, ϵ_∞ is the high-frequency permittivity, τ is the relaxation time, and ω is the radiated frequency.

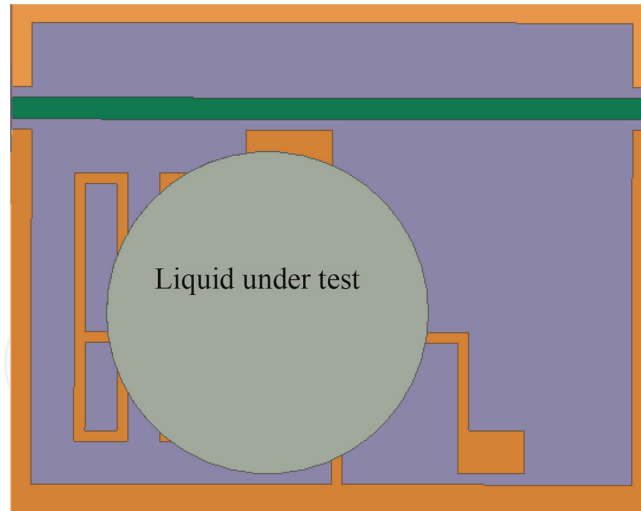


Figure 13.
 Electromagnetic sensor loaded with liquid.

$$\epsilon' = \epsilon_{\infty} + \frac{\epsilon_s - \epsilon_{\infty}}{1 + \omega^2\tau^2} \quad (6)$$

Due to the values' stability of the permittivity around 1.5 GHz, the dispersion is not taken into account. We can express the sensor sensitivity by:

$$S = \frac{f_o - f_1}{f_o d\epsilon_r} \quad (7)$$

where f_o is the lower frequency of sensor (1.065 GHz) and f_1 is a upper frequency of sensor (1.195 GHz), and $d\epsilon_r$ is the variation in the relative permittivity from volume fraction of 10–100%, which is considered of (79–9.5 = 69.5), from **Table 3**. The simulated sensitivity has a maximum value given as:

$$(1.195 - 1.065) / (1.195 \times 69.5) = 0.156\%$$

A sensitivity of 0.156%, which is acceptable compared with the literature in [29, 35, 37, 39, 40], given respectively as 0.11%, 0.27%, 0.54%, 0.26%, and 0.14%. The

	Ethanol	ϵ'	ϵ''
100%	0%	79.0	9.2
90%	10%	73.0	11.3
70%	30%	58.5	17.1
50%	50%	43%	17.1
30%	70%	29.0	16.0
10%	90%	15.5	12
0%	100%	9.5	8.1

Table 3.
 References values of complex permittivity with mixture of volume fraction water-ethanol [23], at about 2 GHz.

sensitivity of the sensor could be improved by various implementations of metamaterial structures, even by adding electromagnetic band gap (EBG) structures at the top side, or defected ground at the bottom side of the sensor.

6. Conclusions

In this chapter, a great attention was given to the metamaterial structures, split ring resonators (SRRs), complementary split ring resonators (CSRRs), and complementary right-left hand (CRLH) structures, based on transmission lines technologies and zero-order resonators (ZORs). The study has included historical view on the metamaterials' appearance, development, and application. Physical properties of metamaterials have also been discussed, and different types of MTMs have been introduced, with MGN permeability negative, ENG negative dielectric, and DNG double-negative electric and magnetic components.

The first application of metamaterial was given to an ultrawide-band monopole antenna loaded with zero-order resonators (ZORs), the antenna could be used in WLAN, WiMax, and X band applications. The proposed antenna was designed and compared with three types of ZOR antenna of similar types. The computed results show that, when loading the monopole antennas with ZOR, the gain reaches 1.8 dBi, and the impedance bandwidth is improved by 148% compared with the original antenna. It was shown that the resonant frequency can be shifted toward lower or higher operating frequencies just by changing the inductor length or adjusting the capacitor value.

The second application is a very compact sensor based on CRLH resonator and CSRR, the sensor is designed for liquid mixture identification, the simulation is done on the commercial software HFSS, three types of liquid mixture are tested on this sensor, and these are ethanol, methanol, and distilled water. The obtained results have shown that the sensitivity of the sensor is very acceptable compared with the literature, and the dimension of the sensor is very compact as well as the testing surface of the sensor.

Finally, metamaterials have the ability of improving the performances of any microwave structures, and this can be done by increasing the gain or the impedance bandwidth of antennas or improving the sensitivity of electromagnetic sensors.

IntechOpen

Author details


Mohamed Lashab^{1*}, Mounir Belattar², Sekkache Hocine² and Halfaya Ahmed¹

1 Laboratory of Electronics and New Technology (LENT), University Larbi Ben M'Hidi, Oum El-Bouaghi, Algeria

2 University of 20 Aout, LARES Laboratory, Skikda, Algeria

*Address all correspondence to: lashabmoh@yahoo.fr

IntechOpen

© 2022 The Author(s). Licensee IntechOpen. This chapter is distributed under the terms of the Creative Commons Attribution License (<http://creativecommons.org/licenses/by/3.0>), which permits unrestricted use, distribution, and reproduction in any medium, provided the original work is properly cited. 

References

- [1] Milligan TA. *Modern Antenna Design*. 2nd ed. New Jersey: Wiley & sons; 2005
- [2] Balanis CA. *Antenna Theory, Analysis and Design*. 4th ed. New Jersey: Wiley & Sons; 2016
- [3] Crosswell WF, Bailey MC. In: Johnson RC, Jasik H, editors. *Antenna Engineering Handbook*. New York: McGraw-Hill; 1984
- [4] Fujimoto K, James JR. *Mobile Antenna Systems Handbook*. 2nd ed. Boston: Artech House; 2001
- [5] Tsoulos G. *MIMO Systems Technology for Wireless Communication*. New York: Taylor Francis; 2006
- [6] Lashab M, Zebiri C-E, Djouablia L, Belattar M, Saleh A, Benabdelaziz F, et al. Characterization of horn antenna loaded with CLL unit cell. *Microwave and Optical Technology Letter*. 2018;**60**(8):1847-1856
- [7] Hocine S, Lashab M, Ouchtati S. Design of sensor based on CRLH for liquid mixture application. In: *ICEECA'19 4th International Conference on Electrical Engineering Control Application*. Constantine Algeria; 2019
- [8] Lashab M, Kosha J, Abdussalam FM, Belattar M, Djouablia L, Zebiri CE, et al. Design and Optimization of Electromagnetic Sensor Based On CRLH Resonator. Loughborough, UK; 2018
- [9] Jan NA, Lashab M, Zebiri CE, Linda D, Abd-Alhameed RA, Benabdelaziz F. Compact CPW antenna loaded with CRLH-TL and EBG for multi-band and gain enhancement. In: *Loughborough Antennas & Propagation Conference*. Loughborough, UK: LAPC. 2016
- [10] Ramsay J. Microondas antenna de guía de ondas y técnicas antes de 1900. *Actes de l'IRE (Abstracto)*. 1958;**46**(2):405
- [11] Brown J. Artificial dielectrics. *Progress in Dielectrics*. 1960;**2**:195-225
- [12] Kock WE. Metal-lens antennas. *Proceedings of IRE*. 1946;**34**:828-836
- [13] Shelby R et al. Experimental verification of a negative index of refraction. *Science*. 2001;**292**:77-79
- [14] Lamb H. On group-speed. *Proceedings of London Mathematical Society*. 1904;**1**:473-479
- [15] V. Veselago. "The electrodynamics of substances with simultaneously negative values of ϵ and μ ," *Soviet Physics Uspekhi*, vol. 10, no. 4, pp. 509–514, Jan., Feb. 1968
- [16] Pendry JB. Negative refraction makes a perfect lens. *Physical Review Letters*. 2000;**85**(18):3966-3969
- [17] Caloz C, Itoh T. Novel microwave devices and structures based on the transmission line approach of metamaterials. In: *IEEE-MTT Int'l Symp.* Philadelphia, PA; 2003. pp. 195-198
- [18] A. Sanada, C. Caloz, and T. Itoh. "Characteristics of the composite right/left-handed transmission lines," *IEEE Microwave Wireless Components Letters*, vol. 14, no. 2, pp. 68–70, February 2004
- [19] Caloz C, Sanada A, Itoh T. A novel composite right/left-handed coupled-line directional coupler with arbitrary

coupling level and broad bandwidth. *IEEE Transactions on Microwave Theory and Technology*. 2004;**52**(3):980-992

[20] Engheta N, Ziolkowski RW. *Metamaterials, Physics and Engineering Explorations*. Canada: Wiley & Sons; 2006

[21] D. R. Smith, W. J. Padilla, D. C. Vier, S. C. Nemat-Nasser, and S. Schultz. "Composite medium with simultaneously negative permeability and permittivity," *Physical Review Letters*, vol. 84, no. 18, pp. 4184–4187, May 2000

[22] Smith DR, Schurig D. Electromagnetic wave propagation in media with indefinite permittivity and permeability tensors. *Physical Review Letters*. 2003;**90**:077405

[23] Bao J-Z, Swicord ML, Davis CC. Microwave dielectric characterization of binary mixtures of water, methanol, and ethanol. *Journal of Chemical Physics*. 1996;**104**(12):22

[24] Lashab M et al. *Electrically Small Planar Antennas Based on Metamaterial: Antenna Fundamentals for Legacy Mobile Applications and Beyond*. Springer International Publishing AG; 2018. pp. 71-98. DOI: 10.1007/978-3-319-63967-3_4

[25] Sabah C, Uckun S. Multilayer system of Lorentz-Drude type Metamaterials with dielectric slabs and its application to electromagnetic Filters. *Progress in Electromagnetics Research*. 2009;**91**: 349-364

[26] Smith DR, Shultz S, Markos P, Soukoulis CM. Determination of effective permittivity and permeability of Metamaterials from reflection and transmission coefficients. *Physical Review B*. 2002;**65**:1951041-1951045

[27] Chen X, Grzegorzczak TM, Wu BI, Pacheco J, Kong JA. Robust method to retrieve the constitutive effective parameters of metamaterials. *Physical Review E*. 2004;**70**:016608

[28] Lubkowski G, Schuhmann R, Weiland T. Extraction of effective metamaterial parameters by parameter fitting of dispersive models. *Microwave Optic Technology Letters*. 2007;**49**(2): 285-288

[29] Saeed K, Pollard RD, Hunter IC. Substrate integrated waveguide cavity resonators for complex permittivity characterization of materials. *IEEE Transaction on Microwave Theory and Techniques*. 2008;**56**(10):2340-2347

[30] Chi Y-J, Chen F-C. Compact CPW-based zeroth-order Resonant Antenna with interleaving CRLHD unit cells. *Progress in Electromagnetics Research C*. 2013;**40**:119-130

[31] Wang G, Feng Q. A novel coplanar waveguide feed zeroth-order resonant antenna with resonant ring. *IEEE Antennas and Wireless Propagation Letters*. 2014;**13**:774-777

[32] Lashab M, Jan NA, Zebiri C. *The I shape Antenna Loaded with ZOR For WLAN and WiMax Application*. Loughborough; 2015

[33] Chaozhu Zhang, Jing Zhang and Lin Li, "Triple band-notched UWB antenna based on SIR-DGS and fork-shaped stubs," *Electronics Letters* 16th January 2014 Vol. 50 No. 2 pp. 67–69

[34] Withawat Withayachumnankul, Kata Jaruwongrungruee, Christophe Fumeaux and Derek Abbott, "Metamaterial-inspired multichannel thin-film sensor," *IEEE Sensors Journal*, Vol. 12, No. 5, May 2012

[35] Ebrahimi A, Withayachumnankul W, Al-Sarawi S, Abbott D. High-sensitivity metamaterial-inspired sensor for microfluidic dielectric characterization. *IEEE Sensors Journal*. 2014;**14**(5)

[36] Horestani AK, Naqui J, Abbott D, Fumeaux C, Martín F. Two-dimensional displacement and Alignment sensor based on reflection Coefficients of open microstrip lines loaded with split ring resonators. *Electronics Letters*. 2014; **50**(8):620-622

[37] Benkhaoua L, Benhabiles MT, Riabi ML. Miniaturized quasi-lumped resonator for dielectric characterization of liquid mixtures. *IEEE Journal & Magazine*. 2016;**16**(6):1603-1610

[38] Albishi AM, Ramahi OM. Microwaves-based high sensitivity sensors for crack detection in metallic materials. *IEEE Transaction on Microwave Theory and Techniques*. 2017;**65**(5):1864-1872

[39] Chretiennot T, Dubuc D, Grenier K. "A microwave and microfluidic planar resonator for efficient and accurate complex permittivity characterization of aqueous solutions," *Microwave Theory and Techniques*, *IEEE Transactions on*. Feb 2013;**61**(2):972,978

[40] Gennarelli G, Romeo S, Scarfi MR, Soldovieri F. A microwave resonant sensor for concentration measurements of liquid solutions. *Sensors Journal IEEE*. 2013;**13**(5):1857

[41] Hocine S, Mohamed Lashab M, Belattar SO, See CH, Yim-Fun H, Abd-Alhameed RA. Microwave sensor for liquid mixture identification based on composite right left hand-zero-order resonator for sensitivity improvement. *International Journal of RF and Micro Computer Aided Engineering*. Wiley; 2022;**32**(11):1456-1465